Electronic Supplementary Material (ESI) for Journal of Materials Chemistry A.

An Electron-Rich 2-Alkylthieno[3,4-*b*]thiophene Building Block with Excellent Electronic and Morphological Tunability for High-Performance Small-Molecule Solar Cells

Shengjie Xu, ‡[a, c] Zichun Zhou, ‡[a,c] Haijun Fan,[a] Longbin Ren,[a,c] Feng Liu, *[,b,d] Xiaozhang Zhu,*[,a,c] and Thomas P. Russell[d,e]

[a] Beijing National Laboratory for Molecular Sciences, CAS Key Laboratory of Organic Solids, Institute of Chemistry, Chinese Academy of Sciences, Beijing 100190, China. E-mail: xzzhu@iccas.ac.cn

[b] Department of Physics and Astronomy, Shanghai Jiaotong University, Shanghai 200240, China. E-mail: iamfengliu@gmail.com

[c] University of Chinese Academy of Sciences, Beijing 100049, China

[d] Polymer Science and Engineering Department, University of Massachusetts, Amherst, Massachusetts 01003, United States

[e] Materials Sciences Division, Lawrence Berkeley National Laboratory, Berkeley, CA 94720, United States

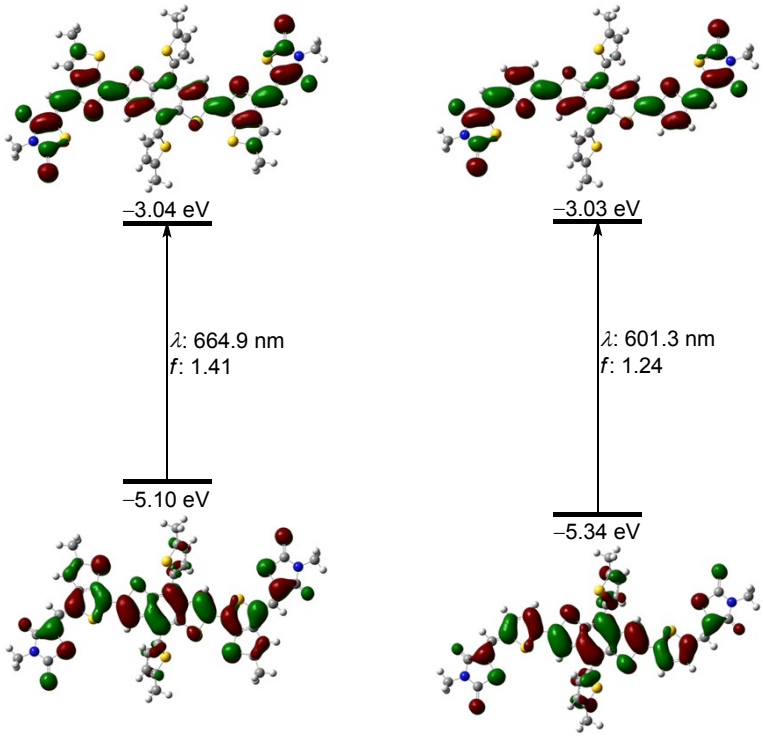

Fig. S1 DFT-calculated orbital energy diagram and pictorial representation of frontier orbitals for STB-n (STB-1: R^1 = *n*-octyl, R^2 = ethyl; STB-2: R^1 = EH, R^2 = ethyl; STB-3: R^1 = EH, R^2 = methyl) and the reference compound STB-r (EH = 2-ethylhexyl, HD = 2-hexyldecyl). Calculations were conducted at the DFT//B3LYP/6-31G** level. Alkyl substituents were replaced by methyl groups to simplify the calculations.

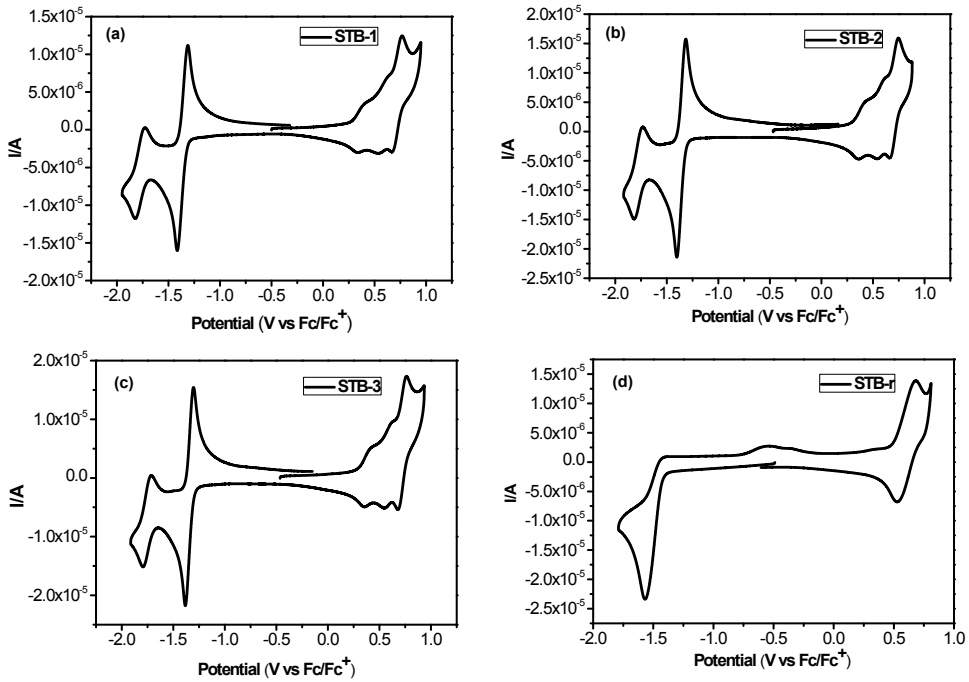

Fig. S2 Cyclic voltammogram of (a) STB-1, (b) STB-2, (c) STB-3, and (d) STB-r in diluted CH_2Cl_2 solution with a scan rate of 100 mV s^{-1}.

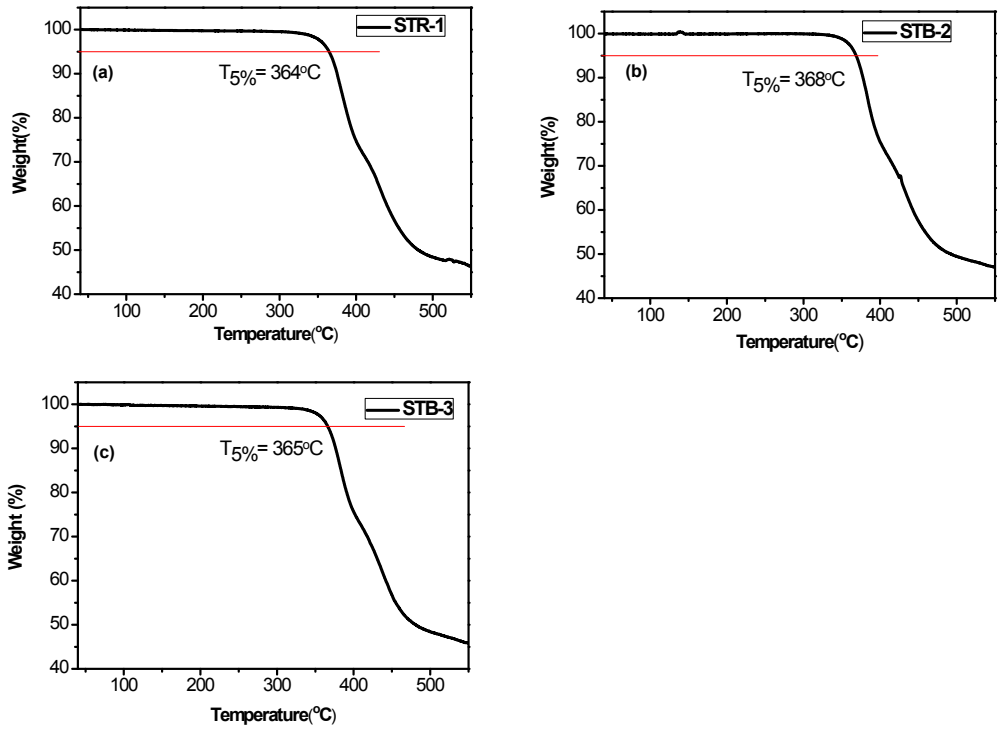

Fig. S3 Thermal gravimetric analysis (TGA) curves of compounds (a) STB-1, (b) STB-2, and (c) STB-3.

Table S1. Photovoltaic performance of STB-n-based solar cells with different thicknesses with device structure of ITO/PEDOT:PSS/active layer/Ca/Al[a]

Cpd.	Thickness (nm)	V_{oc} (V)	J_{sc} (mA cm^{-2})	Fill factor (FF)	PCE (%)
STB-1	80	0.935	10.55	0.64	6.30
	100	0.938	11.20	0.63	6.61
	120	0.938	10.87	0.63	6.42
STB-2	80	0.900	13.82	0.66	7.34
	100	0.901	13.12	0.66	7.84
	120	0.906	12.84	0.67	7.79
STB-3	80	0.917	12.85	0.70	8.24
	100	0.921	13.03	0.71	8.47
	120	0.923	12.79	0.71	8.38

[a] With $CHCl_3$ vapor annealing.

Table S2. Photovoltaic performance of STB-3-based solar cells with different thicknesses with device structure of ITO/PEDOT:PSS/active layer/PFN/Al[a]				
Thickness (nm)	V_{oc} (V)	J_{sc} (mA cm^{-2})	Fill factor (FF)	PCE [%]
80	0.925	13.66	0.72	9.09
120	0.928	14.24	0.70	9.26
140	0.933	14.18	0.68	9.01
160	0.931	13.82	0.69	8.87
[a]With $CHCl_3$ vapor annealing.				

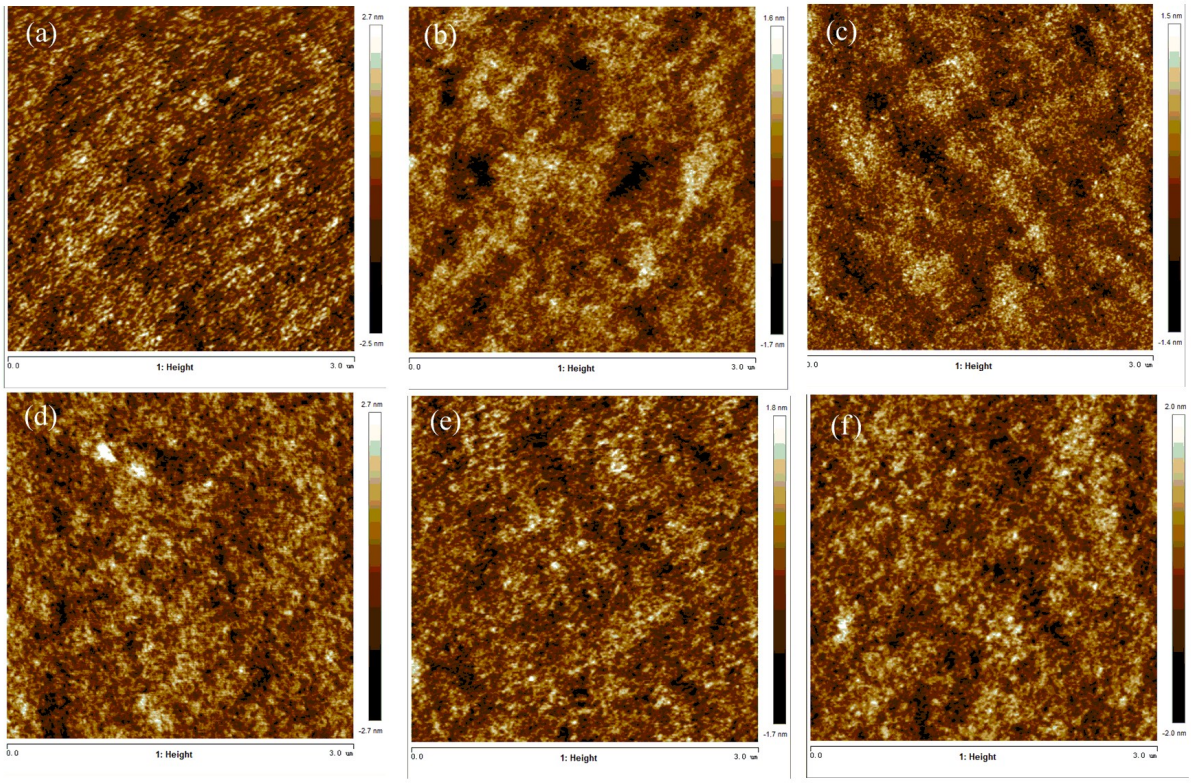

Fig. S4 Tapping-mode AFM height images of optimal blend films cast from chloroform solution: (a) STB-1:$PC_{71}BM$, the RMS roughness is 0.75 nm. (b) STB-2:$PC_{71}BM$, the RMS roughness is 0.47 nm. (c) STB-3:$PC_{71}BM$, the RMS roughness is 0.41 nm. (d) STB-1:$PC_{71}BM$, with SVA treatment, the RMS roughness is 0.77 nm. (e) STB-2:$PC_{71}BM$, with SVA treatment, the RMS roughness is 0.49 nm. (f) STB-3:$PC_{71}BM$, with SVA treatment, the RMS roughness is 0.56 nm. (Atomic force microscope investigation was performed using Bruker MultiMode 8 AFM in "tapping" mode.)

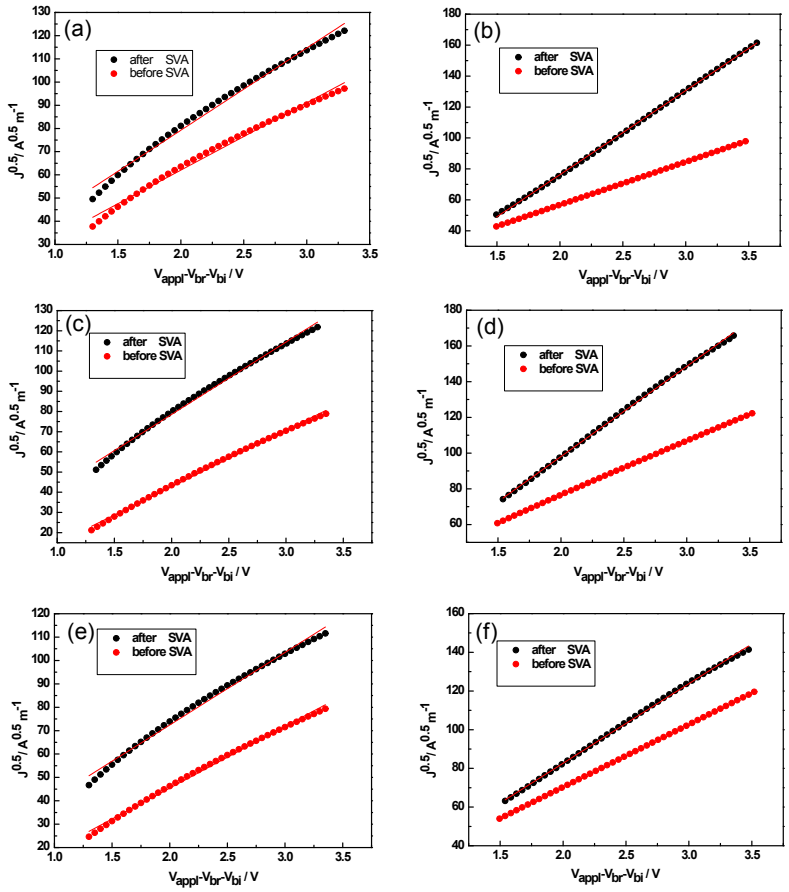

Fig. S5 $J^{0.5}$ vs V plots: STB-1/$PC_{71}BM$ (1:1.5, w/w) hole-only diode (a) and electron-only diode (b), STB-2/$PC_{71}BM$ (1:1.5, w/w) hole-only diode (c) and electron-only diode (d), STB-3/$PC_{71}BM$ (1:1.5, w/w) hole-only diode (e) and electron-only diode (f).

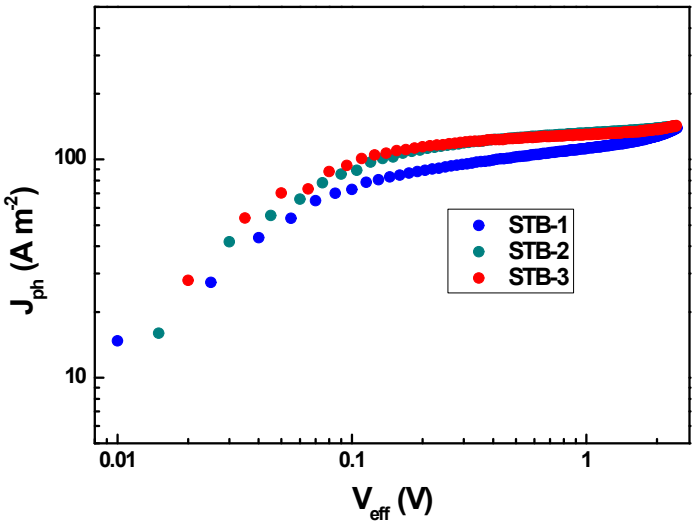

Fig. S6 Photocurrent density versus effective voltage (J_{ph}–V_{eff}) characteristics for three devices under constant incident light intensity (AM 1.5G, 100 mW cm^{-2}).

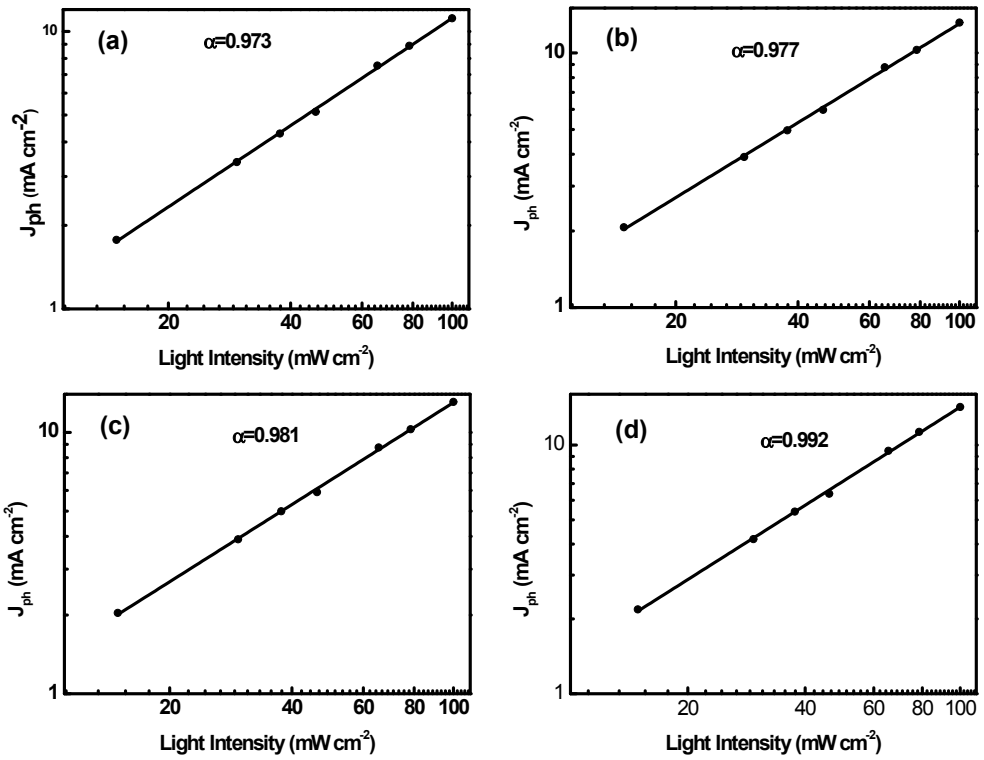

Fig. S7 Measured J_{ph} of STB-1-based (a), STB-2-based (b), STB-3-based (c) and STB-3-based with PFN cathode interlayer (d) solar cells plotted against light intensity on the logarithmic scale.

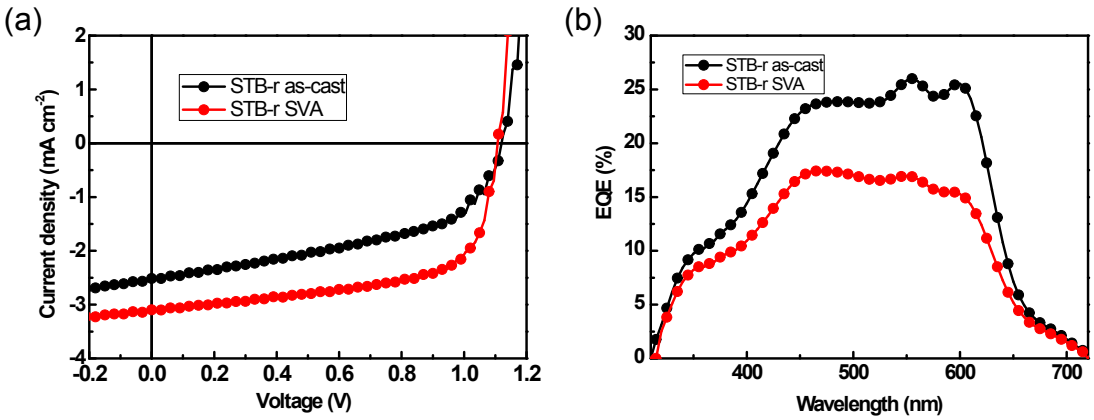

Fig. S8 (a) Characteristic density vs voltage (*J*-*V*) curves and (b) external quantum efficiency (EQE) curves of STB-r.

Table S3. Photovoltaic performance of STB-r-based solar cells with device structure of ITO/PEDOT:PSS/active layer/Ca/Al

Cpd.	Treatment	V_{oc} (V)	J_{sc} (mA cm^{-2})	Fill factor (FF)	PCE (%)
STB-r	none	1.12	2.51	0.49	1.39
	SVA[a]	1.11	3.25	0.64	2.24

[a]With $CHCl_3$ vapor annealing.

NMR Charts

6,6′-(4,8-Bis(5-(2-ethylhexyl)thiophen-2-yl)benzo[1,2-*b*:4,5-*b*′]dithiophene-2,6-diyl)bis(2-octylthieno[3,4-*b*]thiophene-4-carbaldehyde) (6)

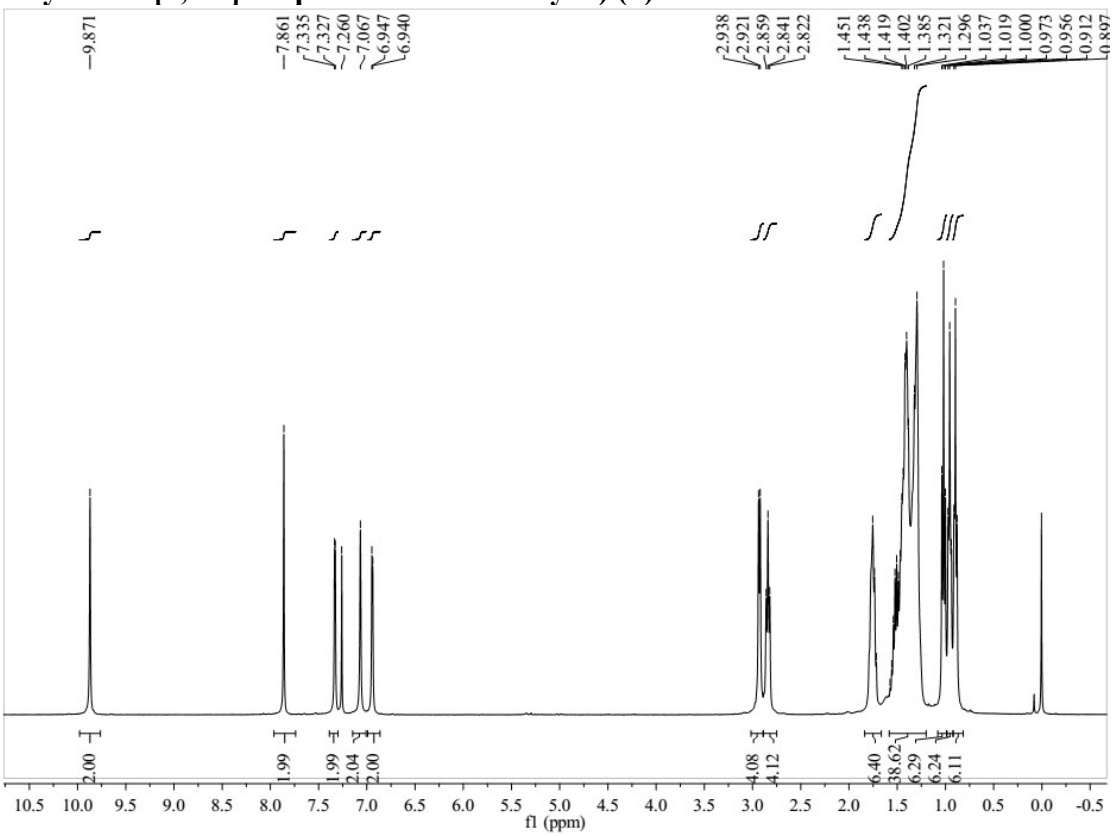

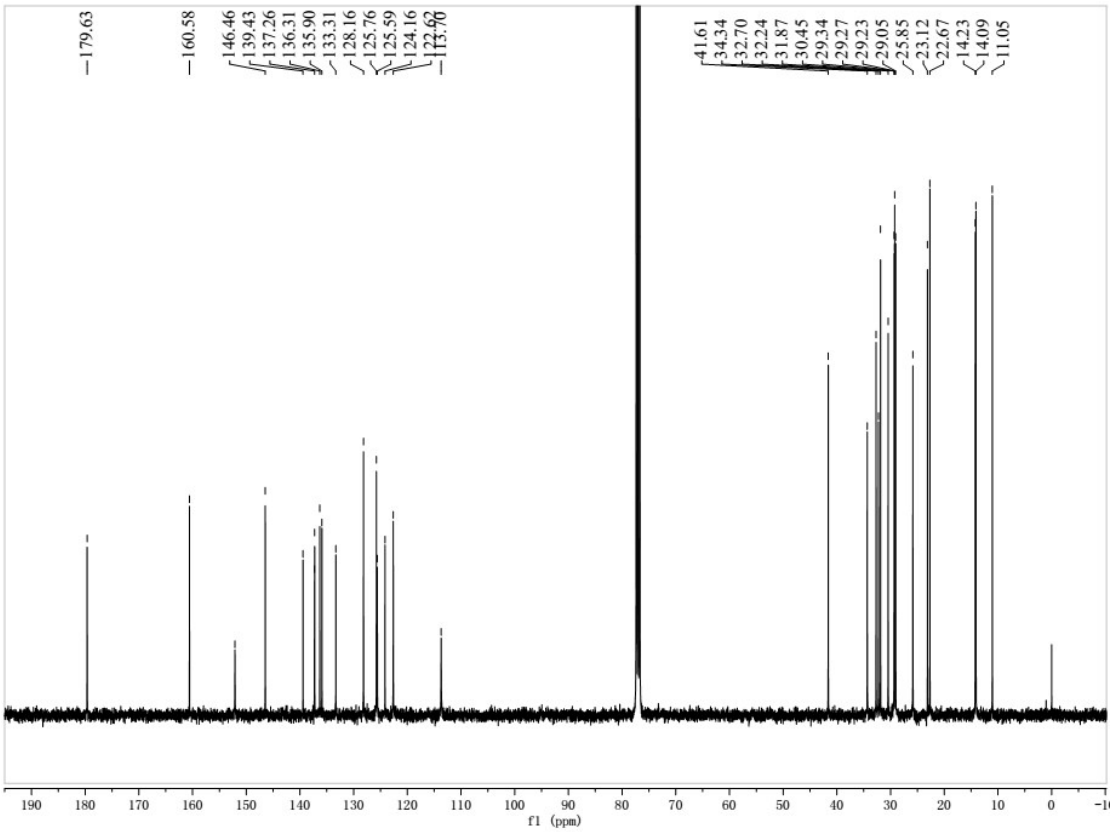

6,6′-(4,8-Bis(5-(2-ethylhexyl)thiophen-2-yl)benzo[1,2-*b*:4,5-*b*′]dithiophene-2,6-diyl)bis(2-(2-ethylhexyl)thieno[3,4-*b*]thiophene-4-carbaldehyde) (7)

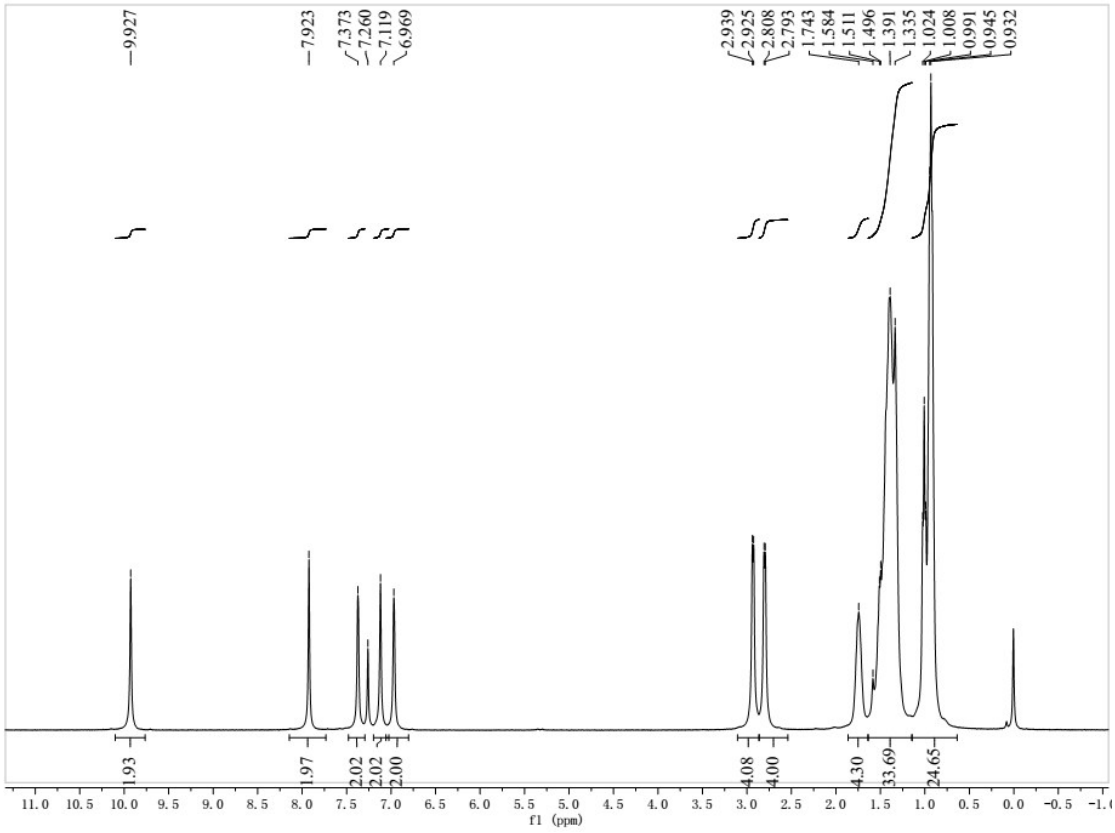

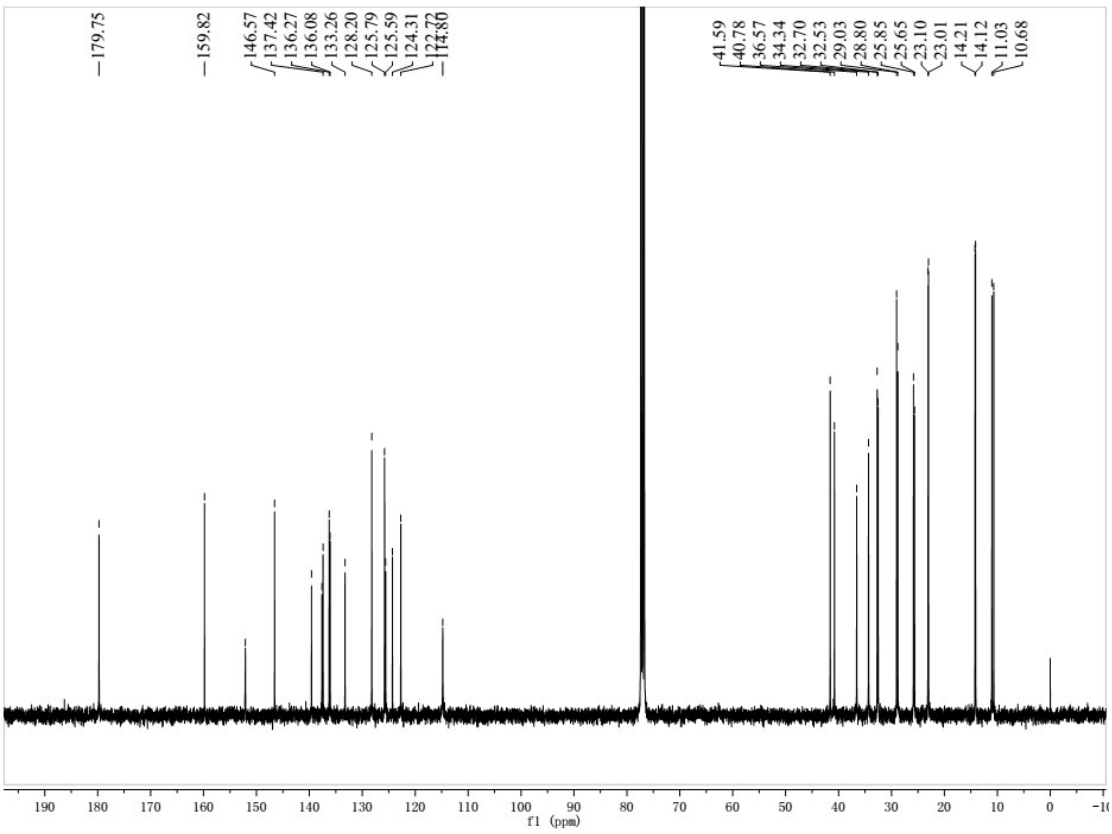

(5*Z*,5′*Z*)-5,5′-((6,6′`-(4,8-bis(5-(2-ethylhexyl)thiophen-2-yl)benzo[1,2-*b*:4,5-*b*′]dithiophene-2,6-diyl)bis(2-octylthieno[3,4-*b*]thiophene-6,4-diyl))bis(methanylylidene))bis(3-ethyl-2-thioxo-thiazolidin-4-one) (STB-1)

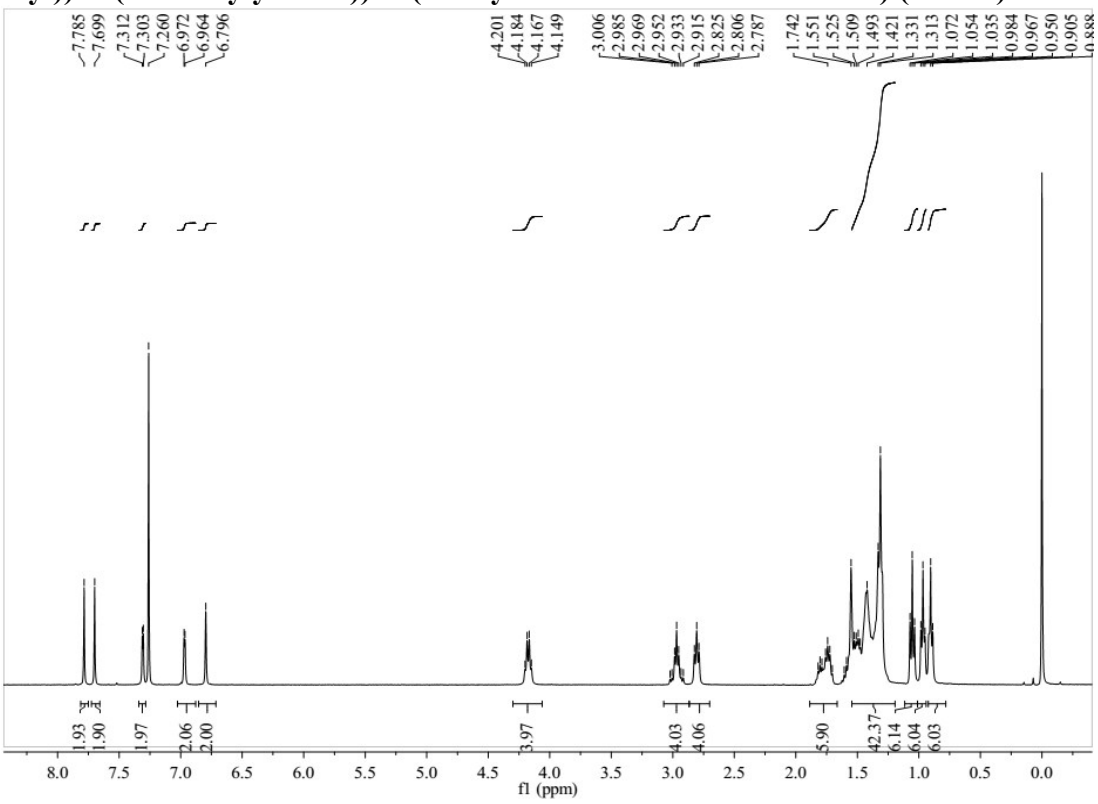

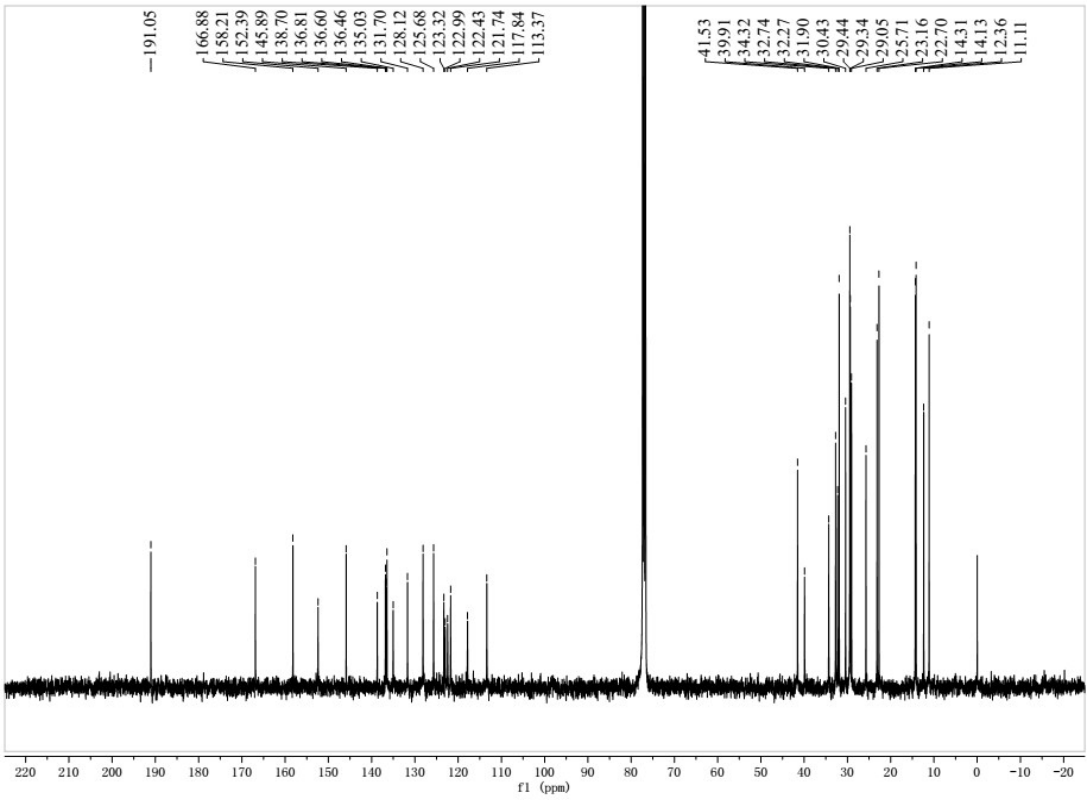

(5*Z*,5′*Z*)-5,5′-((6,6′-(4,8-Bis(5-(2-ethylhexyl)thiophen-2-yl)benzo[1,2-*b*:4,5-*b*′]dithiophene-2,6-diyl)bis(2-(2-ethylhexyl)thieno[3,4-*b*]thiophene-6,4-diyl))bis(methanylylidene))bis(3-ethyl-2-thioxothiazolidin-4-one) (STB-2)

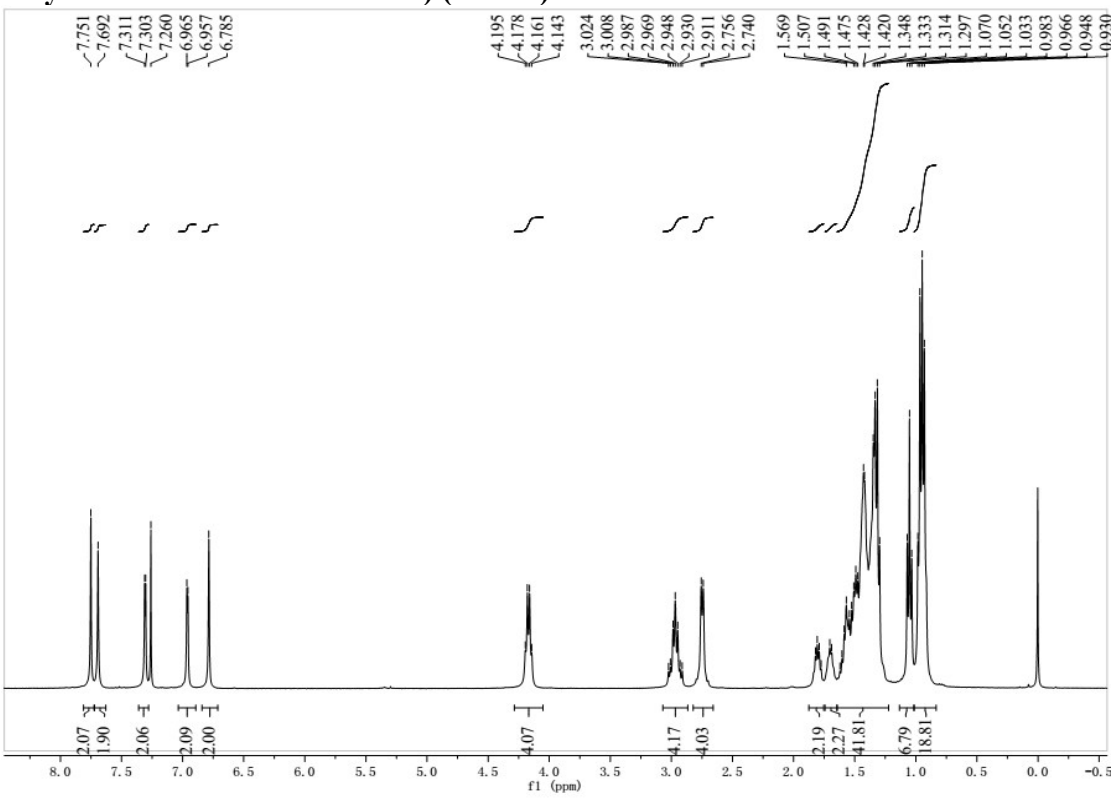

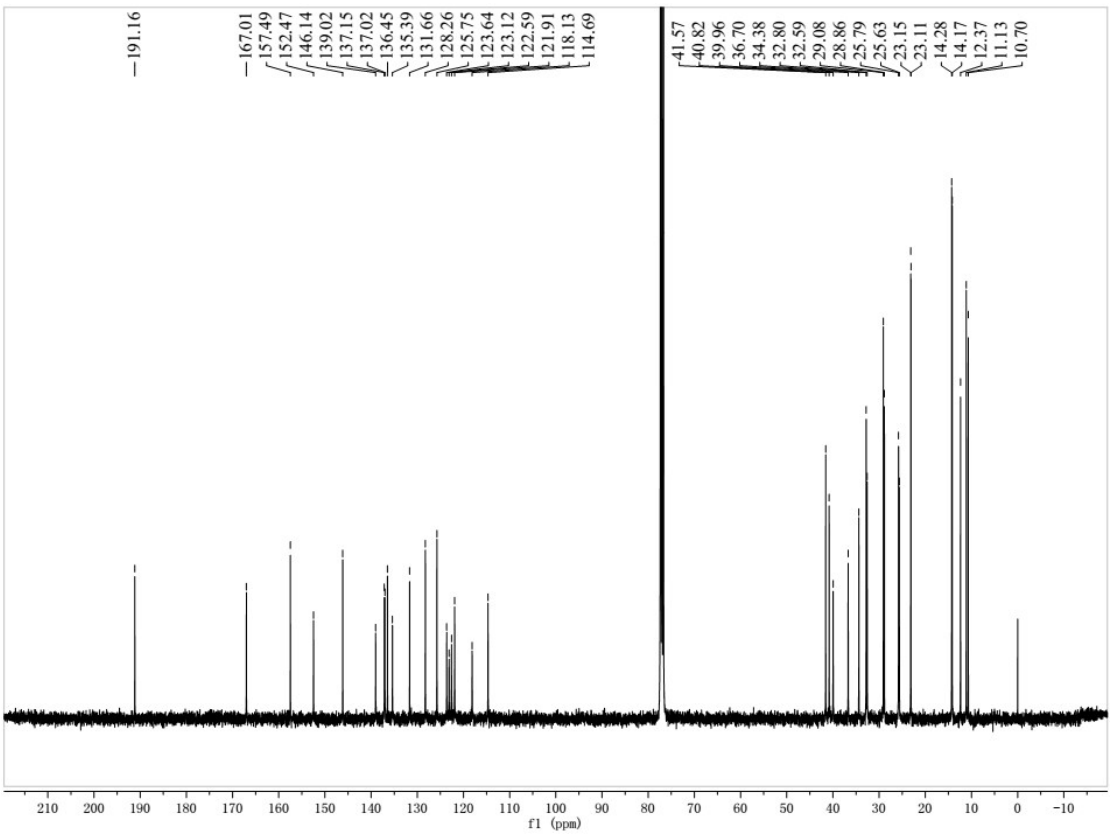

(5*Z*,5′*Z*)-5,5′-((6,6′-(4,8-Bis(5-(2-ethylhexyl)thiophen-2-yl)benzo[1,2-*b*:4,5-*b*′]dithiophene-2,6-diyl)bis(2-(2-ethylhexyl)thieno[3,4-*b*]thiophene-6,4-diyl))bis(methanylylidene))bis(3-methyl-2-thioxothiazolidin-4-one) (STB-3)

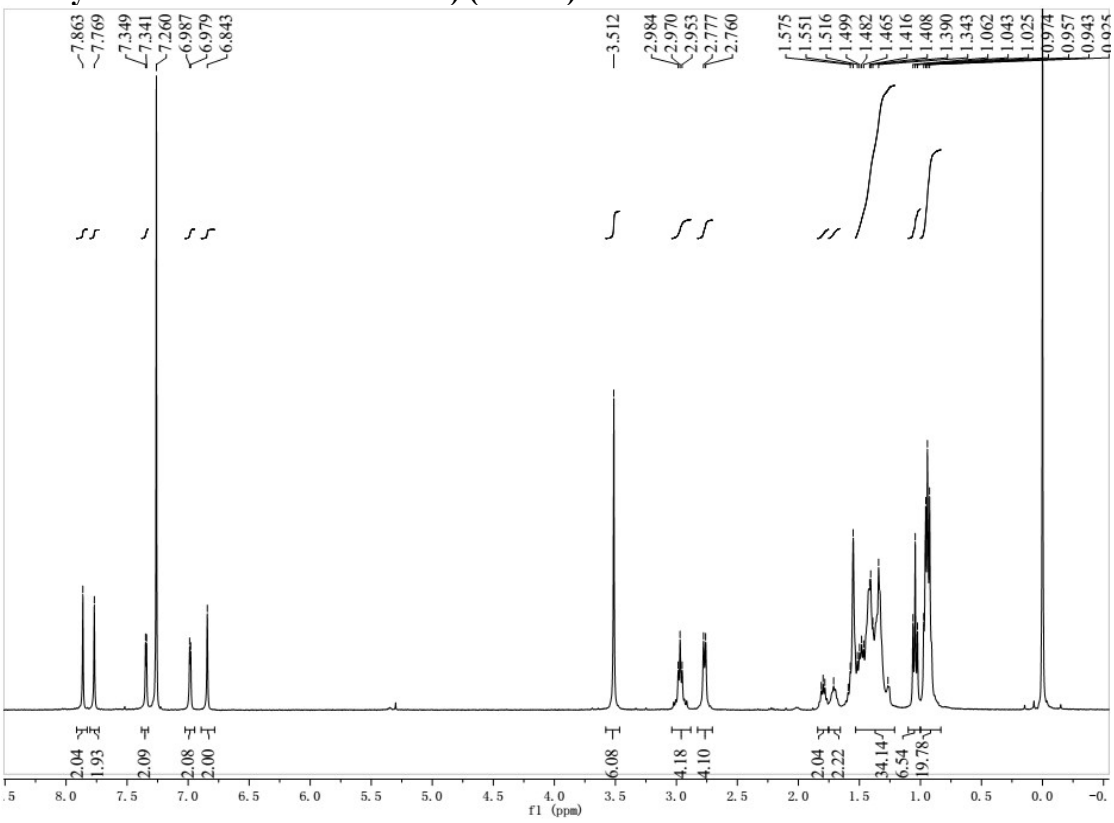

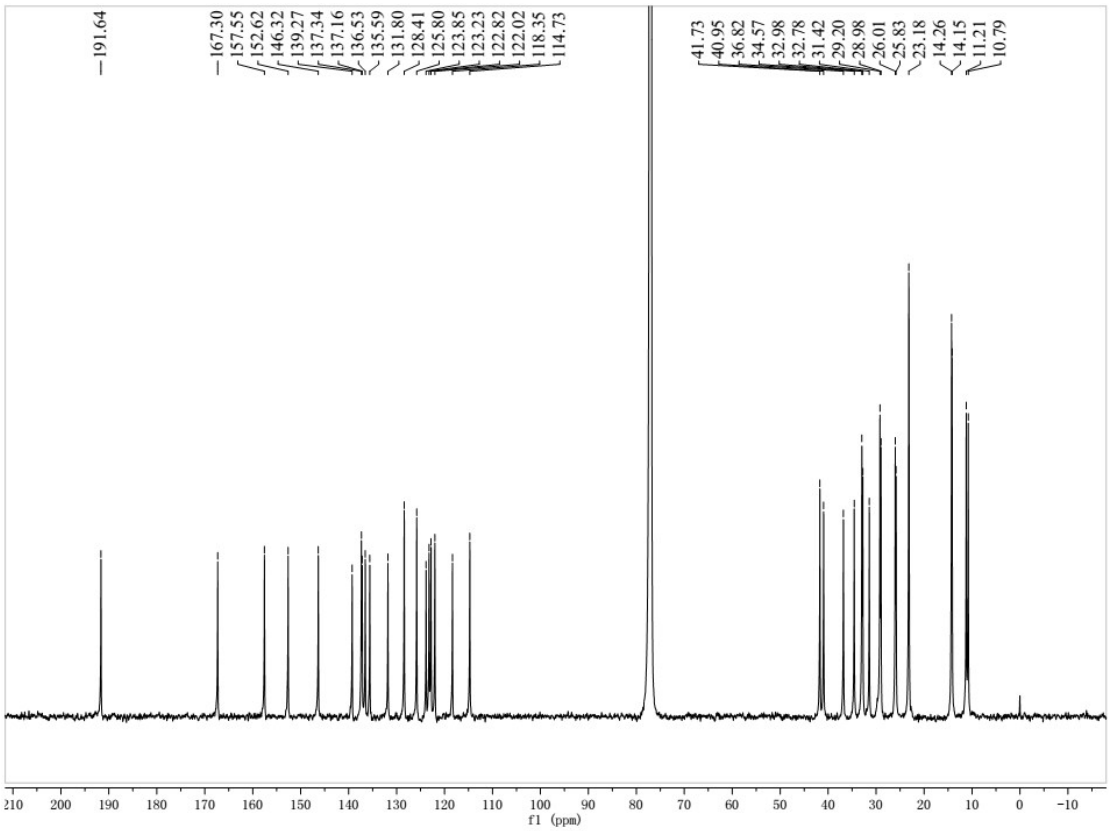

(5*Z*,5′*Z*)-5,5′-((5,5′-(4,8-Bis(5-(2-hexyldecyl)thiophen-2-yl)benzo[1,2-*b*:4,5-*b*′]dithiophene-2,6-diyl)bis(thiophene-5,2-diyl))bis(methanylylidene))bis(3-octyl-2-thioxothiazolidin-4-one) (STB-r)

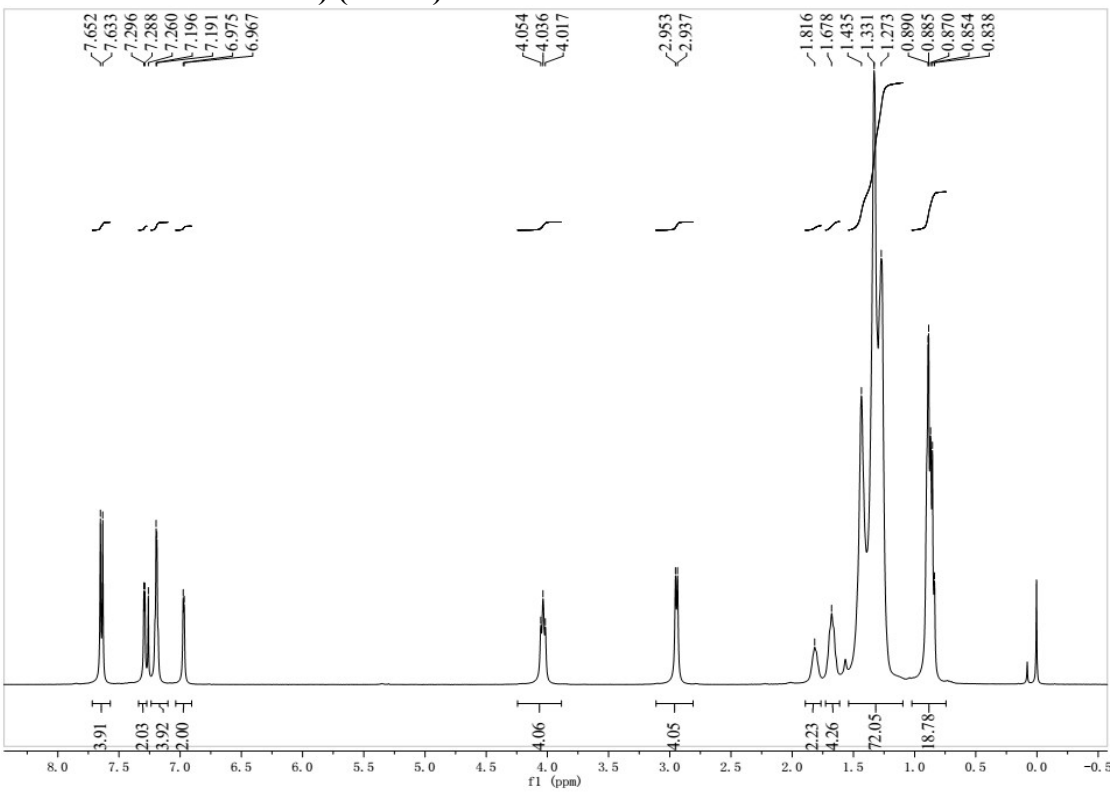

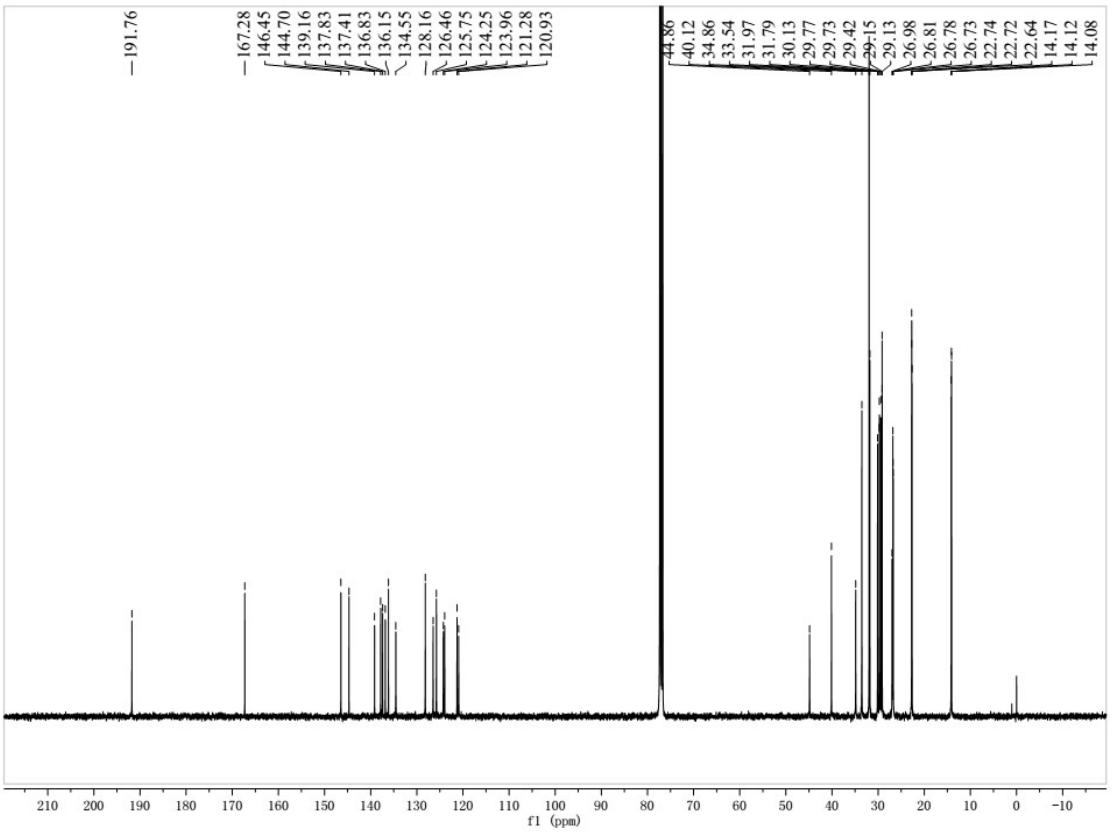

MALDI-TOF Mass Spectrum of STB-1

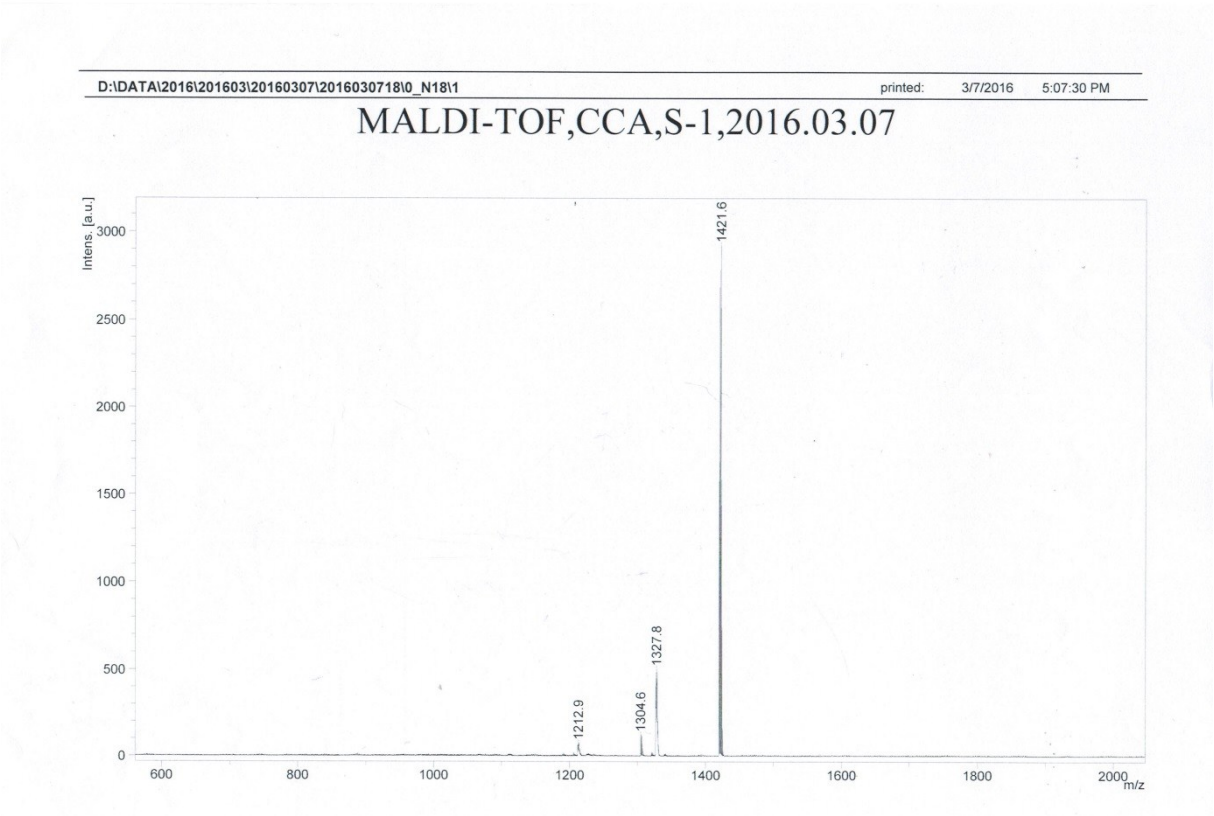

MALDI-TOF Mass Spectrum of STB-2

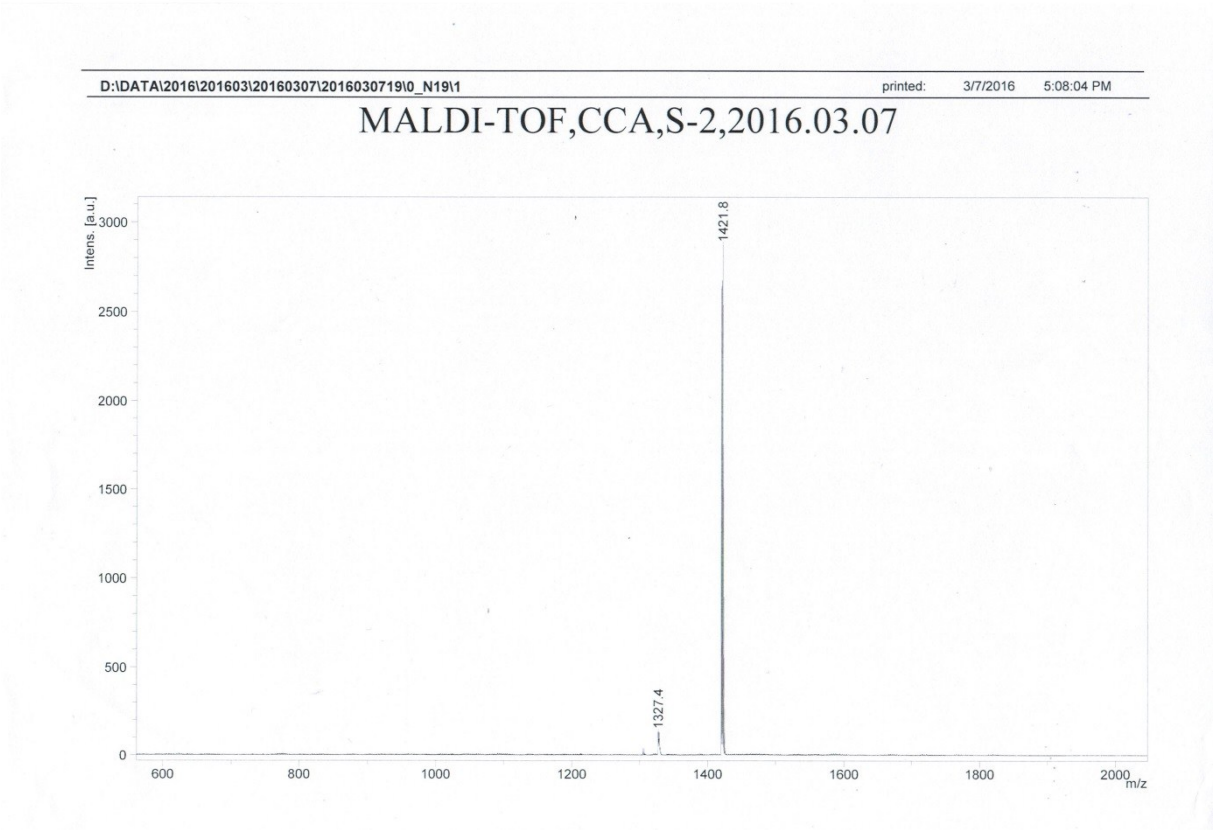

MALDI-TOF Mass Spectrum of STB-3